Ocean Sci. Discuss., 3, 585–608, 2006
www.ocean-sci-discuss.net/3/585/2006/

Ocean Science
Discussions

Papers published in *Ocean Science Discussions* are under
open-access review for the journal *Ocean Science*

Operational analysis of the circulation and shelf-slope exchanges in the continental margin of the northwestern Mediterranean

A. Jordi, G. Basterretxea, A. Orfila, and J. Tintoré

IMEDEA (CSIC-UIB), Institut Mediterrani d'Estudis Avançats, Esporles, Illes Balears, Spain

Received: 31 March 2006 – Accepted: 8 May 2006 – Published: 21 June 2006

Correspondence to: A. Jordi (vieaajb@uib.es)

Abstract

In this paper, we present the results from a high horizontal resolution numerical simulation of the northwestern Mediterranean using a z-level, non-hydrostatic, primitive equation ocean model (DieCAST). The high resolution allows an accurate representation of the submarine canyons that presides in the region. The model is one-way coupled to a large scale model of the Mediterrenean Sea through open boundaries and uses the atmospheric forcing fields provided in terms of HIRLAM outputs by the Spanish National Institute of Meteorology. Results show that the model can successfully reproduce the complex general circulation characteristics of the area, including the modificacions induced by canyons in their vicinity and other phenomena observed such as instabilities and coastal trapped waves. The sea surface temperature is similar to satellite observations except that simulated temperatures are slightly warmer near the coast than observations and colder near the open boundaries. An important topic of this work is the computation of the shelf-slope exchanges, which are able to renew shelf waters in a few months.

1 Introduction

Shelf-ocean interactions are receiving increasing attention because of their enormous importance in aspects such as climate change, global biogeochemical cycles, marine ecosystems, resource exploitation and other human related activities. Much of the present understanding about shelf-slope exchanges derives from processes oriented studies carried out since the late 70s. It is not until recently that the oceanographic community has developed reliable tools to provide nowcasts and forecasts of marine environmental conditions, in support of a variety of activities at sea. This endeavor has become possible both by the improvement of operational systems able to incorporate and analyze data in real time and by the progress in modelling and computing capabilities. An example of theses efforts in providing operational information is the

European project MFSTEP (Mediterranean Forecasting System Toward Environmental Predictions) which is focused on the Mediterranean Sea.

Observational and modelling based analysis of the Mediterranean reveal a complex and variable circulation that is strongly affected by frontal dynamics through mesoscale features (Millot, 1999; Send et al., 1999; Demirov and Pinardi, 2002). This variability is the result of interactions at basin, sub-basin and local scales that results in intense mesoscale variability. In the Mediterranean Sea, mesoscale and even sub-mesoscale and local processes have profound impact on ocean dynamics and, consequently, in ocean geochemistry and ecosystems (e.g. Levy et al., 2001). The necessity of predictive tools resolving processes at these scales encompasses an integral view of the ocean system and the use of nested schemes that allow for downscaling from general to local conditions.

The northwestern Mediterranean Sea is one of the areas of interest of the European cooperative oceanography project MFSTEP where nested operational models have been implemented. This region comprises the shelves and slopes of the Gulf of Lions and the Catalan Sea (Fig. 1). Bottom topography in the area is rather complex, varying form a broad shelf in the Gulf of Lions to a rather narrow continental margin in the Catalan Sea. The slope is indented by a series of canyons that cut across about 60% of the slope area (Álvarez et al., 1996). Submarine canyons in the Gulf of Lions occur as deep and short indentations of the shelf edge separated by narrow open slopes. Conversely, the Palamós and Blanes canyons in the Catalan shelf are more prominent and expand to the proximity of the coast.

The major aspects of the water mass structure and flow dynamics of this region are fairly well known and have been thoroughly described by several authors (e.g. Millot, 1999). The general circulation is dominated by a cyclonic along-slope density front, called the Northern Current, flowing from northeast to southwest (Font et al., 1988). Previous studies have found that this current is characterized by relevant spatial and temporal variability, with a large variety of mesoscale features (such as meanders and instabilities) strongly interacting with the basin-scale circulation (La Violette et al., 1990). These instabilities have been observed to evolve into very energetic filaments and shedding eddy-like structures (Wang et al., 1988; Tintoré et al., 1990). In addition, very intense ocean-atmosphere interaction mechanisms, characterized by strong episodes of northerly winds, have been described in this area (Korres et al., 2000).

The complex topography and the strong dynamical processes that characterize the Northwestern Mediterranean provide a good opportunity to analyze the effect of physical transport processes on the shelf-slope exchanges of water, solutes and particles. In this context, the objectives of the present paper are twofold: (1) to validate the ocean forecast model implemented in the continental margin of the northwestern Mediterranean in the basis of previous knowledge and available data, and (2) to provide estimations of the shelf-slope exchanges resulting from the interaction between the Northern Current and the topographic irregularities under real forcing conditions.

2 Model description

For the purpose of this study, the Dietrich/Center for Air-Sea Technology (DieCAST) ocean model was operationally run for the northwestern Mediterranean at high horizontal resolution following a downscaling approach from a basin-scale model of the Mediterranean Sea. DieCAST is a z-level, non-hydrostatic, primitive equation ocean model (Dietrich, 1997; Dietrich and Lin, 2002), which provides high computational accuracy and low numerical dissipation and dispersion (Dietrich et al., 2004). The model uses a rigid lid approximation, with a sea surface pressure formulation, and the Boussinesq approximation. The governing equations are solved using a blend of collocated and staggered grid structures (Arakawa A and C grids) and fourth-order-accurate control volume approximation for the horizontal pressure gradient and advection terms, except in zones adjacent to boundaries where conventional second order accuracy is used (Sanderson, 1998; Sanderson and Brassington, 1998). The solution of the non-hydrostatic equation is obtained iteratively from the hydrostatic solution, as described in more detail in (Dietrich and Lin, 2002).

OSD

3, 585–608, 2006

Simulations are run with horizontal viscosity and diffusivity coefficients set to a constant value of 10 m^2/s. For the vertical viscosity and diffusivity, a variable formulation which includes the Richardson number is used, as described and used in Staneva et al. (2001), with background values set at near-molecular values (10^{-6} and $2 \cdot 10^{-7}$ m^2/s respectively). The bottom dissipation is represented by a conventional nonlinear bottom drag with a coefficient of $2 \cdot 10^{-3}$. At the lateral walls we assume free-slip boundary condition. The DieCAST model has been recently used to study the regional circulation in the vicinity of the Monterey Submarine Canyon (Haney et al., 2001; Tseng et al., 2005) and to study the mesoscale, seasonal and interannual variability in the Mediterranean Sea (Fernández et al., 2005).

2.1 Model domain

The model domain includes the continental margins of the Gulf of Lions and the Catalan Sea (northwestern Mediterranean) extending from 41.2° N to 43.6° N in latitude and from 1.5° E to 5.6° E in longitude (Fig. 1). The model horizontal resolution is $0.75'$, which is equivalent to 1389 m in the meridional direction and up to 1036 m in the zonal direction. Note that the Coriolis parameter f is variable and, in consequence, the resolution in the zonal direction is not constant (although the variation is not significant). The bathymetry on the model grid is derived from the bathymetric chart of the northwestern Mediterranean (http://www.icm.csic.es/geo/gma/MCB) by a bilinear interpolation without filtering or smoothing. In the vertical, the model grid has 30 non uniform vertical levels concentrated towards the surface with the top layer thickness being 10 m, and increasing smoothly to 300 m at the bottom.

2.2 Initialization and boundaries

The model is one-way coupled to a large scale model through the open boundaries of the domain. The open boundaries allow perturbations generated inside the computational domain to leave it without deterioration of the inner model solution and allows

OSD
3, 585–608, 2006
Operational analysis of NW Mediterranean shelf
A. Jordi et al.

physically important external information to advect inward using a pure upwind advective scheme (Tseng et al., 2005). Results from the global Mediterranean Sea model (Tonani et al., 2006) are used to force the two lateral open boundaries (south and east) and all quantities are interpolated from daily global Mediterranean model output and updated every time step (150 s). The global Mediterranean model results on 1 December 2005 are used to initialize the model by interpolation of the horizontal velocity components, temperature and salinity. The model runs for 30 days between 1 December 2005, 00:00:00 UTC and 31 December 2005, 00:00:00 UTC.

2.3 Atmospheric forcing

At the sea surface, the model is driven by the wind stress and surface fluxes provided by the Spanish National Institute of Meteorology in terms of 3 hourly fields of the High Resolution Limited Area Model (HIRLAM, http://hirlam.org). The horizontal resolution of wind forcing at 10 m above the surface and net heat and water fluxes is 0.16°. There is no relaxation of the surface temperature or salinity.

To provide a general picture of the evolution of wind forcing at 10 m, temporal variance complex EOF modes and corresponding amplitude functions are computed. The spatial pattern and its corresponding amplitude functions of the most relevant EOF are shown in Fig. 2a. This pattern accounts for 64.4% of the total variance of the data, while the second mode (not shown) account for 11.3%. The spatial distribution is characterized by a northwesterly wind blowing in the entire basin, with maximum speeds offshore.

The amplitude functions describe the dynamics of the spatial modes (Fig. 2b). During the first days the wind blows from the southwest and it progressively rotates clockwise to the northeast increasing the intensity. Vector velocities exceeding 12 m/s were registered between 8 and 15 December 2005, rotating to the northwest at the end of this period. A secondary peak from the northwest was observed in lasts days of December.

OSD

3, 585–608, 2006

3 Results and discussion

3.1 General circulation

A temporal average of surface circulation over the integration period based on 6-hourly model outputs reproduces the characteristic features of the circulation in northwestern Mediterranean Sea. Along the shelf break, the flow is constrained to follow the topography and strong currents (>40 cm/s) develop cyclonically flowing from the Gulf of Lions to the Catalan Sea (Fig. 3). This feature is consistent with descriptions of the Northern Current although current velocities are above reported values of 20–30 cm/s (Send et al., 1999). However it should be noted that, as mentioned above, strong northeasterly winds were experienced during a significant part of the analyzed period.

Another conspicuous structure is the presence of an anticyclonic eddy to the south of the model domain (between 4° E and 5° E). Anticyclonic eddy formation appears to be favored between adjacent coastal upwelling cells on the Gulf of Lions under Mistral forcing (Levy et al., 1990), which was predominant during the model integration period, and the structures tend to be rather persistent. Indeed, Pascual et al. (2002) tracked a similar structure in that position from middle September 1998 to middle March 1999 using a combination of in situ and satellite data. Onken et al. (2005) also describe a strong anticyclonic vortex at about 41° N exhibiting maximum surface flow speeds of up to 65 cm/s, on fall 2002.

Further agreement concerns the impact of topographic irregularities on the Northern Current. It is well known that submarine canyons affect the spatial pattern of regional vertical motions (Hickey, 1997), particularly in subsurface layers. Figure 4 shows the temporal average of vertical velocity at 95 m depth. A close relation between vertical movement and canyons is evidenced with downwelling on the upstream walls of the canyons and upward motions on the downstream edges. This antisymmetrical structure of vertical motions was previously by simulated by Ardhuin et al. (1999) in the Blanes Canyon and by Jordi et al. (2005a) in the Palamós Canyon.

3.2 Frontal structures and coastal trapped waves

The southwestern propagation of meanders and eddies along the slope, associated with the Northern Current has been frequently observed moving along the slope in the Gulf of Lions and Catalonia (La Violette et al., 1990; Tintoré et al., 1990). Meanders of about 30–40 km propagating at phase speeds of 5–15 km/day that grow as filaments and develop into isolated eddies have been reported (Flexas et al., 2002; Rubio et al., 2005). Similar southwestward-propagating frontal structures are observed in the present simulation. Figure 5 reveals several meanders propagating along the slope. Southward propagation at phase speeds of about 9 km/day was estimated from visual analysis of the complete image set (not shown). Off the slope of the Gulf of Lions (3.9° E, 42.8° N) a filament with a mushroom-like structure (B) develops during the analyzed period.

The model is also able to reproduce coastal trapped waves which propagate cyclonically along the continental margins of the Gulf of Lions and the Catalan Sea. The presence of coastal trapped waves in the area have been recently identified by Jordi et al. (2005b) using alongshore currents and sea level time series. The time evolution of the sea level anomaly (SLA) predicted by the model along the 100 m isobath in the Catalan Sea is shown in Fig. 6. In spite that SLA contours are disturbed by small scale features, they present a constant slope that evidences the southwestward propagation of disturbances. The phase speed of these disturbances is about 250 cm/s, which corresponds to the phase speed of the first coastal trapped wave mode in the area.

3.3 Comparison with observation data

Satellite images of sea surface temperature provide a useful tool to test the performance of numerical results in the upper ocean. A monthly averaged SST image of the study area, for December 2005, was obtained from the German Aerospace Research Center (DLR). Figure 7 shows the comparison between predicted sea surface temperature and observed data. With some exceptions (i.e. local warming in the northeastern

OSD

3, 585–608, 2006

edge of the domain) the large-scale pattern matches well with observations. Obviously, satellite temperature displays small-scale variability that is not captured by the model where all the features appear smeared. The model's temperature along the coast is generally warmer than the observations probably because of the lack of riverine inputs in the model. The location of the anticyclonic eddy in the model (C1) is displaced to the northeast and presents a slightly colder core than satellite values (C2).

An alternative tool to check the model performance of temperature and salinity predictions in the water column is the set of Argo floats (http://www.argo.ucsd.edu/). Figure 8 compares the predicted temperature and salinity profiles with those measured by Argo floats (see Fig. 1 for the location). At deeper levels, both modelled and observed fields are very similar, however, discrepancies appear in the mixing layer. On 4 December 2005, these differences are of the order of 0.2°C in temperature and 0.03 in salinity. On 14 and 29 December 2005, observed surface temperature and salinity are cooler and saltier, respectively. Although further analysis is required, these discrepancies could be attributed to errors on the atmospheric forcing or to inaccuracies on the model's heat transfer between the atmosphere and the ocean.

3.4 Shelf-slope exchange

To study the shelf-slope exchanges, we compute horizontal transports across a vertical plane formed by the shelf break (defined by the 200 m isobath) and its projection on the surface. Horizontal transport is estimated by integrating the cross-slope velocity across this plane with positive transport being directed offshore. According to Dinniman et al. (2003), the cross-slope velocity at each individual grid point along the shelf break is calculated as

$$U_{\text{cross}}=\boldsymbol{U}\cdot\left(\frac{\nabla H}{\nabla H}\right) \quad (1)$$

where $\boldsymbol{U}$ is the horizontal velocity vector and H is the bathymetry.

OSD
3, 585–608, 2006

Figure 9 shows the cross-slope transport, during December 2005, through the vertical plane formed by the projection of the shelf-break. Despite that the cross-slope transport is very close to zero at several locations, clear enhancements occur related to the location of submarine canyons, in particular along the Catalan shelf. Furthermore, onshore and offshore flows are observed on the upstream and downstream side of the canyons respectively. This effect of submarine canyons on cross-shelf transports has been previously observed and modelled by several authors (Skliris et al., 2002; Jordi et al., 2005a). The maximum cross-shelf transport occurs in the vicinity of the Palamós Canyon, which is the most prominent canyon of the area.

As suggested by Fig. 9, the cross-shelf transports are greater in the period from 8 to 15 December 2005. A budget of the volume transport across the shelf-break confirms this point and shows good correspondence with the amplitude function of the most relevant EOF from the u-component of wind forcing (Fig. 10). During this wind enhanced period, larger transports correspond to winds from the northeast. This is in agreement with the results of Ardhuin et al. (1999) for the Blanes Canyon. In fact, the combined effects of canyon topography and of the wind forcing during energetic storms are responsible for a large increase of both cross-shore and vertical transports (Skliris et al., 2004). Recently, a large increase in downward particle fluxes was measured in the Palamós Canyon during a severe storm with northeasterly winds (Palanques et al., 2005).

The total volume of water transported from the shelf to the open ocean during the integration period reached $10.8 \cdot 10^{12}$ m^3. Similarly, the volume transport from the open ocean to the shelf is estimated to be $9.2 \cdot 10^{12}$ m^3 and hence a net offshore transport is suggested by these values. Nevertheless, not all cross-shelf transported water is effectively exchanged (Jordi et al., 2006[1]). since to a large extent these fluxes could correspond to onshore-offshore fluctuations. (Jordi et al., 2006[1]) suggest that only a

[1] Jordi, A., Klinck, J. M., Basterretxea, G., Orfila, A., and Tintoré, J.: Estimation of shelf-slope exchanges induced by frontal instability near submarine canyons, J. Geophys. Res., under review, 2006

half of water transported across the shelf break produces an effective exchange of water. Following this estimation, the effective exchange in the Gulf of Lions and the Catalan Sea for December 2005 would be of about $5 \cdot 10^{12}$ m^3. Assuming a similar magnitude for the entire winter it could be concluded that waters of the Gulf of Lions and the Catalan Sea are completely renewed during this season. This result is consistent with the estimations obtained by Jordi et al. (2005a) for the northwestern Mediterranean and with the values reported by She and Klinck (2000) off Oregon.

4 Conclusions

Within the framework of the MFSTEP, a high-resolution nonhydrostatic model has been developed in the northwestern Mediterranean coupled to a basin-scale Mediterranean Sea model. The numerical study is focused on the continental margins of the Gulf of Lions and the Catalan Sea, where the circulation is dominated by the Northern Current and shelf bathymetry is incised by numerous submarine canyons. The model reproduces well several known features of the general circulation in the area, although slight discrepancies were observed with satellite derived SST and Argo floats measurements in the mixing layer. Deficiencies in the air-sea coupling algorithms and in the atmospheric forcing are suggested as plausible causes for these differences. Major efforts are presently centered in the improvement of atmosphere-ocean couplings and in the development of data assimilation schemes to sequentially update the model forecast with new observations.

A relevant topic of this study is the estimation of shelf-slope exchanges. Volume transports across the shelf-break have been evaluated for December 2005. Our results indicate that submarine canyons contribute significantly to the exchange of water between the continental margin and the open ocean, specially during enhanced wind period. These estimations which suggest that shelf water may be renewed in a few months, are consistent with previously reported values in the vicinity of submarine canyons.

Acknowledgements. This work has been partially supported by ESEOO (VEM200320577C1408) project funded by CYCIT and MFSTEP (EVK3CT200200175) project funded by European Commission (D. G. Research).

References

Álvarez, A., Tintoré, J., and Sabatés, A.: Flow modification of shelf-slope exchange induced by a submarine canyon off the northeast Spanish coast, J. Geophys. Res., 101, 12 043–12 055, 1996. 587

Ardhuin, F., Pinot, J. M., and Tintoré, J.: Numerical study of the circulation in a steep canyon off the Catalan coast, J. Geophys. Res., 104, 11 115–11 135, 1999. 591, 594

Demirov, E. and Pinardi, N.: Simulation of the Mediterranean Sea circulation from 1979 to 1993: Part I. The interannual variability, J. Marine Systems, 33–34, 23–50, 2002. 587

Dietrich, D. E.: Application of a modified Arakawa A grid ocean model having reduced numerical dispersion to the Gulf of Mexico circulation, Dynam. Atmos. Oceans, 27, 201–217, 1997. 588

Dietrich, D. E. and Lin, C. A.: Effects of hydrostatic approximation and resolution on the simulation of convective adjustment, Tellus, Ser. A, 54, 34–43, 2002. 588

Dietrich, D. E., Mehra, A., Haney, R. L., Bowman, M. J., and Tseng, Y. H.: Dissipation effects in North Atlantic Ocean modeling, Geophys. Res. Lett., 31, L05 302, doi:10.1029/2003GL019015, 2004. 588

Dinniman, M. S., Klinck, J. M., and Jr., W. O. S.: Cross-shelf exchange in a model of the Ross Sea circulation and biogeochemistry, Deep-Sea Research II, 50, 3103–3120, 2003. 593

Fernández, V., Dietrich, D. E., Haney, R. L., and Tintoré, J.: Mesoscale, seasonal and interannual variability in the Mediterranean Sea using a numerical ocean model, Prog. Oceanogr., 66, 321–340, 2005. 589

Flexas, M. M., de Madron, X. D., Garcia, M. A., Canals, M., and Arnau, P.: Flow variability in the Gulf of Lions during the MATER HFF experiment (March–May 1997), J. Marine Syst., 33–34, 197–214, 2002. 592

Font, J., Salat, J., and Tintoré, J.: Permanent features of the circulation in the Catalan Sea, Oceanol. Acta, 9, 51–57, 1988. 587

Haney, R. L., Hale, R. A., and Dietrich, D. E.: Offhore propagation of eddy kinetic energy in the California current, J. Geophys. Res., 106, 11 709–11 717, 2001. 589

Hickey, B. M.: The Response of a steep-sided, narrow canyon to a time-variable wind forcing, J. Phys. Oceanogr., 27, 697–729, 1997. 591
Jordi, A., Orfila, A., Basterretxea, G., and Tintoré, J.: Shelf-slope exchanges by frontal variability in a steep submarine canyon, Prog. Oceanogr., 66, 120–141, 2005a. 591, 594, 595
Jordi, A., Orfila, A., Basterretxea, G., and Tintoré, J.: Coastal trapped waves in the northwestern Mediterranean, Continental Shelf Res., 25, 185–196, 2005b. 592
Korres, G., Pinardi, N., and Lascaratos, A.: The ocean response to low frequency interannual atmospheric variability in the Mediterranean Sea, Part I: sensitivity experiments and energy analysis, J. Clim., 13, 705–731, 2000. 588
La Violette, P. E., Tintoré, J., and Font, J.: The surface circulation of the Balearic Sea, J. Geophys. Res., 95, 1559–1568, 1990. 587, 592
Levy, M., Klein, P., and Treguier, A. M.: The Gulf of Lions' hydrodynamics, Continental Shelf Res., 10, 885–894, 1990. 591
Levy, M., Klein, P., and Treguier, A. M.: Impact of sub-mesoscale physics on production and subduction of phytoplankton in an oligotrophic regime, J. Marine Res., 59, 535–565, 2001. 587
Millot, C.: Circulation in the Western Mediterranean Sea, J. Marine Syst., 100, 423–442, 1999. 587
Onken, R., Tintoré, J., Fernández, V., Vizoso, G., Basterretxea, G., and Haley, P.: A forecast system of the Balearic Sea, J. Marine Syst., submitted for publication, 2005. 591
Palanques, A., Garcia-Ladona, E., Gomis, D., Martín, J., Marcos, M., Pascual, A., Puig, P., Emelianov, J.-M. G. M., Guillén, S. M. J., Tintoré, J., Segura, M., Jordi, A., Ruiz, S., Basterretxea, G., Font, J., Blasco, D., and Pagès, F.: A multidisciplinary program to studythe dynamics and the ecology of a northwestern Mediterranean submarine canyon: The Palamós Canyon, Prog. Oceanogr., 66, 89–119, 2005. 594
Pascual, A., Nardelli, B. B., Larnicol, G., Emelianov, M., and Gomis, D.: A case of an intense anticyclonic eddy in the Balearic Sea (western Mediterranean), J. Geophys. Res., 107, 3183, doi:10.1029/2001JC000913, 2002. 591
Rubio, A., Arnau, P. A., Espino, M., Flexas, M. M., Jordà, G., J. Salat, J. P., and Arcilla, A. S.: A field study of the behaviour of an anticyclonic eddy on the Catalan continental shelf (NW Mediterranean), Prog. Oceanogr., 66, 142–156, 2005. 592
Sanderson, B. G.: Order and resolution for computational ocean dynamics, J. Phys. Oceanogr., 28, 1271–1286, 1998. 588

Sanderson, B. G. and Brassington, G.: Accuracy in the context of a control-volume model, Atmos.-Ocean, 36(4), 355–384, 1998. 588

Send, U., Font, J., Krahmann, G., Millot, C., Rhein, M., and Tintoré, J.: Recent advances in observing the physical oceanography of the western Mediterranean Sea, Prog. Oceanogr., 44, 37–64, 1999. 587, 591

She, J. and Klinck, J. M.: Flow near submarine canyons driven by constant winds, J. Geophys. Res., 105, 28 671–28 694, 2000. 595

Skliris, N., Hecq, J. H., and Djenidi, S.: Water fluxes at an ocean margin in presence of a submarine canyon, J. Marine Syst., 32, 239–251, 2002. 594

Skliris, N., Lacroix, G., and Djenidi, S.: Effects of extreme meteorological conditions on coastal dynamics near a submarine canyon, Continental Shelf Res., 24, 1033–1045, 2004. 594

Staneva, J., Dietrich, D. E., Stanev, E., and Bowman, M.: Rim current and coastal eddy mechanisms in an eddy-resolving black sea general circulation model, J. Marine Syst., 31, 137–157, 2001. 589

Tintoré, J., Wang, D.-P., and Violette, P. E. L.: Eddies and thermohaline intrusions of the shelf-slope front off the Northeast Spanish coast, J. Geophys. Res., 95(C2), 1627–1633, 1990. 588, 592

Tonani, M., Pinardi, N., Dobricic, S., and Adani, M.: A High Resolution Free Surface Model on the Mediterranean Sea, Ocean Sci., in preparation, 2006. 590

Tseng, Y.-H., Dietrich, D. E., and Ferziger, J. H.: Regional circulation of the Monterey Bay region: Hydrostatic versus nonhydrostatic modeling, J. Geophys. Res., 110, C09 015, doi:10.1029/2003JC002153, 2005. 589, 590

Wang, D.-P., Vieira, M. E. C., Salat, J., Tintoré, J., and Violette, P. E. L.: A shelf-slope filament off the northeast Spanish Coast, J. Geophys. Res., 46, 321–332, 1988. 588

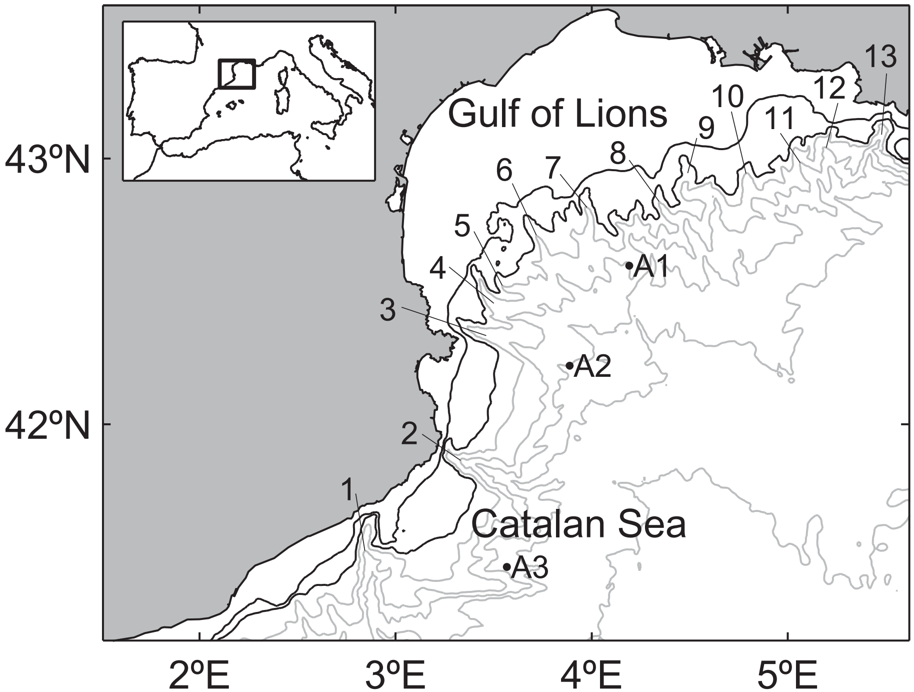

Fig. 1. Model domain of the northwestern Mediterranean and bathymetry. The 100 and 200 m isobaths are plotted with grey lines, and the 500, 1000, 1500, 2000 and 2500 m isobaths with black lines. Black points represent the location of Argo profiles. Numbers indicate prominent submarine canyons: Blanes (1), Palamós (2), Cap de Creus (3), Lacaze-Duthiers (4), Pruyot (5), Boucart (6), l'Hérault (7), Aigüesmortes (8), la Petite Rônne (9), la Grand Rônne (10), Marseille (11), Planier (12), and Cassidaigne (13).

OSD

3, 585–608, 2006

EGU

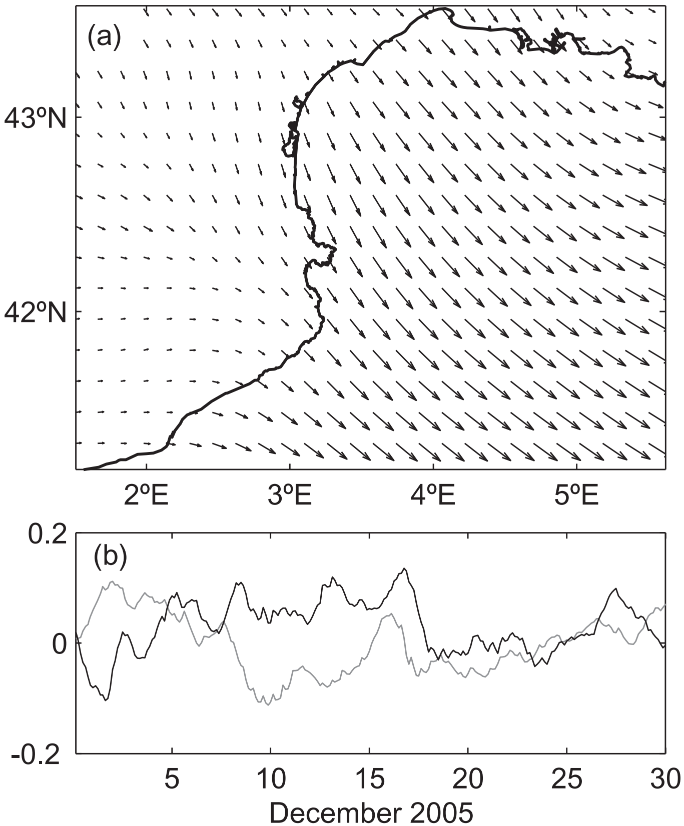

Fig. 2. **(a)** Spatial pattern of the most relevant EOF from the time variability of wind forcing at 10 m. **(b)** Corresponding amplitude functions. The gray line represent the amplitude function for the u-component of the wind forcing, and the black line is the amplitude function for the v-component.

OSD
3, 585–608, 2006

Title Page
Abstract | Introduction
Conclusions | References
Tables | Figures
◀I | ▶I
◀ | ▶
Back | Close
Full Screen / Esc
Printer-friendly Version
Interactive Discussion

EGU

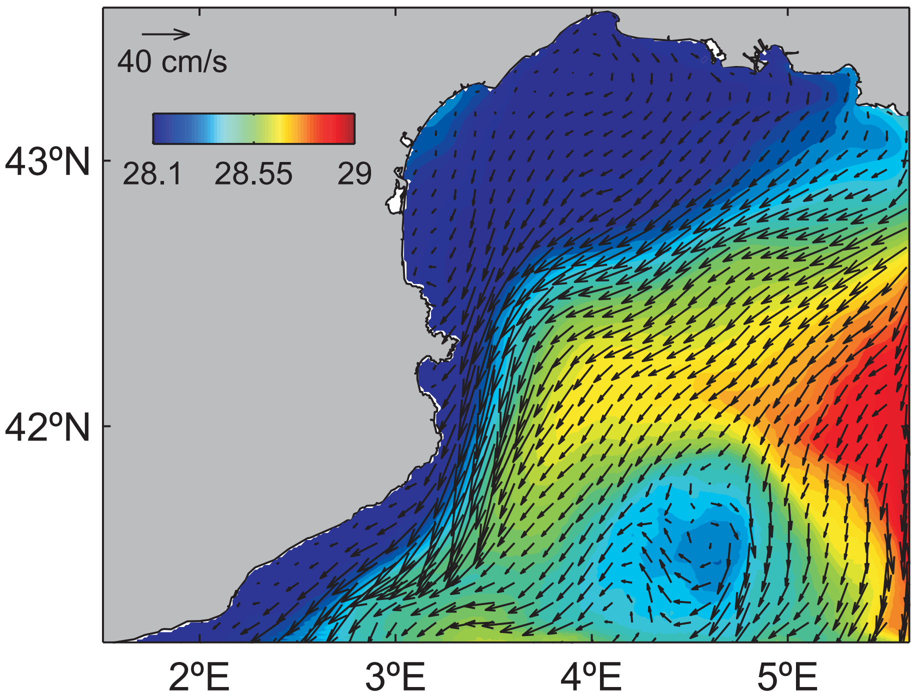

Fig. 3. Time-averaged horizontal velocity and density (σ_t units) at 5 m depth. Vectors are plotted at every eighth grid points.

OSD
3, 585–608, 2006

Operational analysis of NW Mediterranean shelf

A. Jordi et al.

EGU

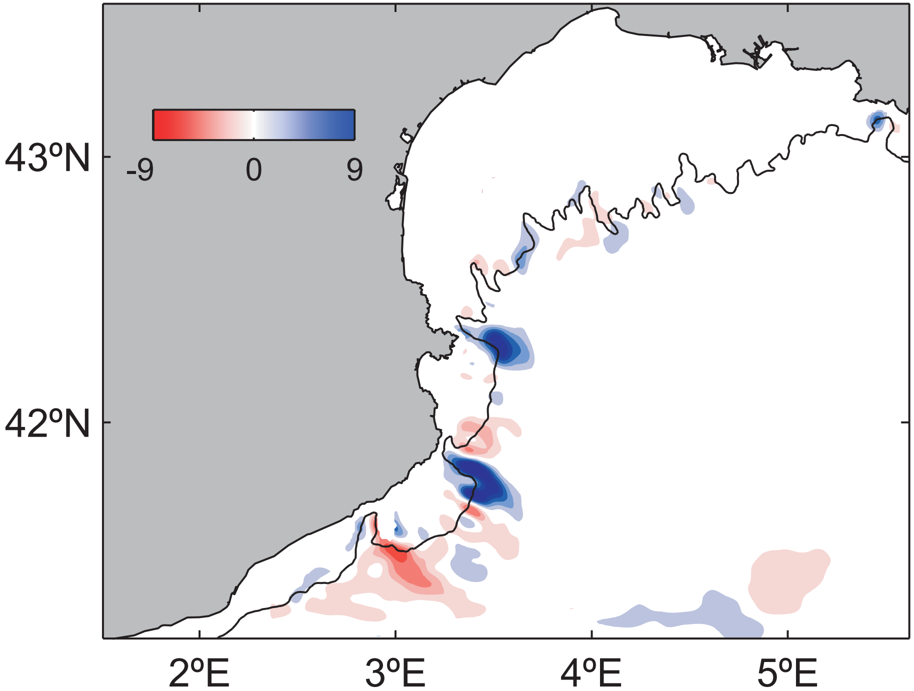

Fig. 4. Time-averaged vertical velocity at a depth of 95 m. The units are m/day. The 200 m isobath is plotted with a black line.

OSD
3, 585–608, 2006

Title Page
Abstract Introduction
Conclusions References
Tables Figures
◀◀ ▶▶
◀ ▶
Back Close
Full Screen / Esc
Printer-friendly Version
Interactive Discussion

EGU

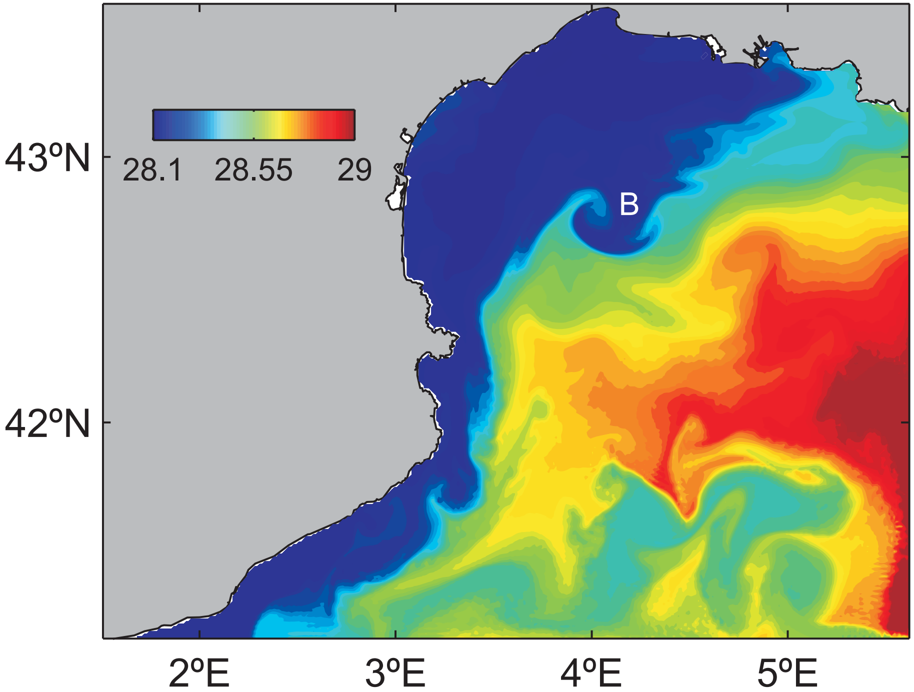

Fig. 5. Surface density (σ_t units) for 23 December 2005. A filament with a mushroom-like structure is indicated with B.

OSD
3, 585–608, 2006

Operational analysis of NW Mediterranean shelf

A. Jordi et al.

Title Page
Abstract | Introduction
Conclusions | References
Tables | Figures
◀| |▶
◀ ▶
Back | Close
Full Screen / Esc
Printer-friendly Version
Interactive Discussion

EGU

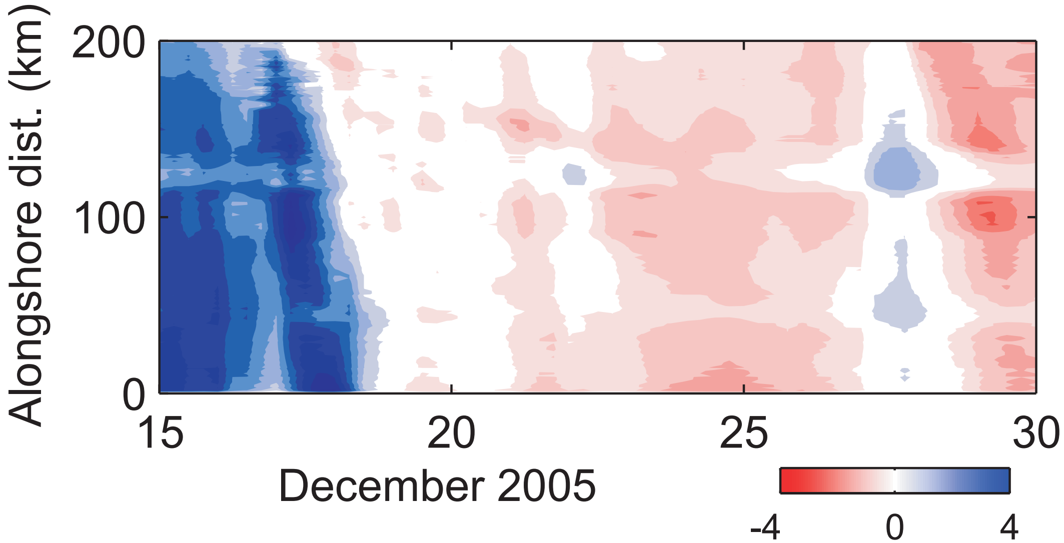

Fig. 6. Evolution of sea level anomaly (SLA, in cm) along the 100 m isobath in the Catalan Sea from 15 to 30 December 2005. The zero along-shore distance is taken at the southernmost point of the 100 m isobath in the model domain. The 200 km along the 100 m isobath corresponds approximately to Cap de Creus, which separates the Catalan Sea and the Gulf of Lions (see Fig. 1).

OSD
3, 585–608, 2006

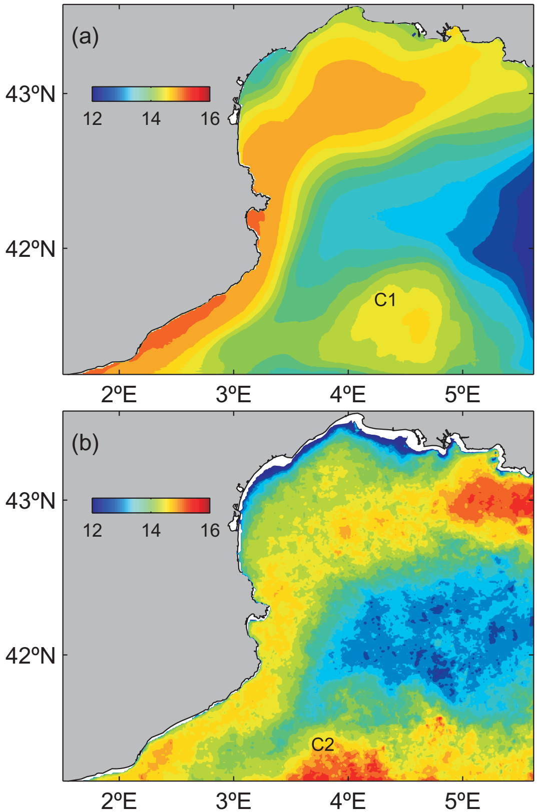

Fig. 7. (a) Time-averaged model surface temperature (˚C). The anticyclonic eddy is indicated with C1. **(b)** Monthly-averaged satellite (AVHRR) SST (˚C) for December 2005. CThe anticyclonic eddy is indicated with C2.

OSD

3, 585–608, 2006

Operational analysis of NW Mediterranean shelf

A. Jordi et al.

EGU

OSD

3, 585–608, 2006

Operational analysis of NW Mediterranean shelf

A. Jordi et al.

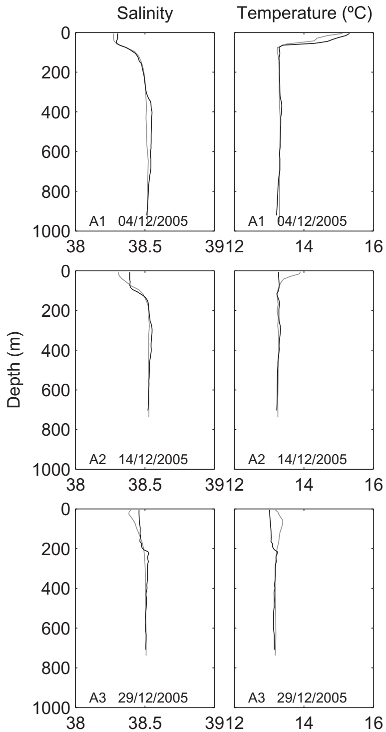

Fig. 8. Comparison between model temperature and salinity profiles (grey line) and those measured by Argo floats (black line). The date of each profile is indicated and its location is shown in Fig. 1.

EGU

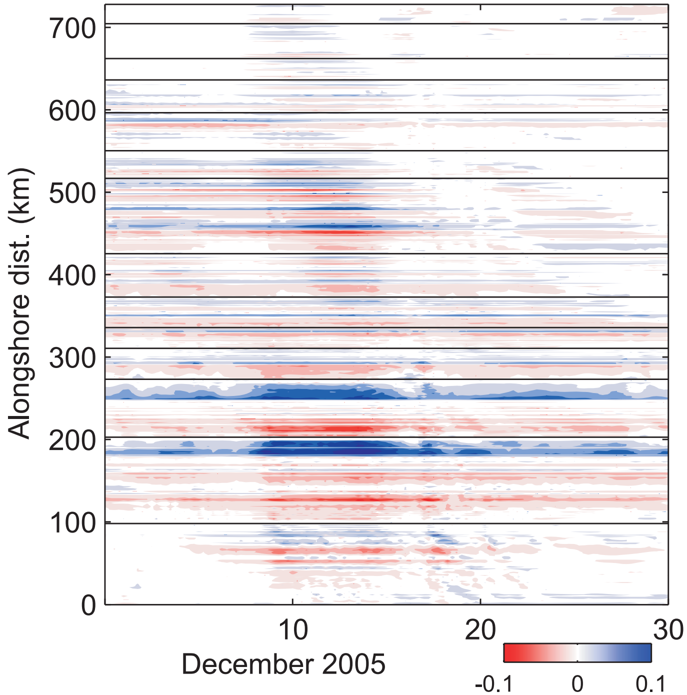

Fig. 9. Transport of volume (Sv) across the shelf break (defined by the 200 m isobath) at each individual grid point along the shelf break. Positive values indicate transport from the shelf to open ocean. The alongshore distance is the distance (in km) following the shelf-break from the southernmost point in the Catalan Sea (0 km) to the eastern edge of the Gulf of Lions at a distance of 720 km. Horizontal black lines represents the location of the canyons heads, which corresponds to the canyons indicated in Fig. 1 (the upper black line is the Cassidaigne Canyon (13) in Fig. 1).

OSD

3, 585–608, 2006

Operational analysis of NW Mediterranean shelf

A. Jordi et al.

EGU

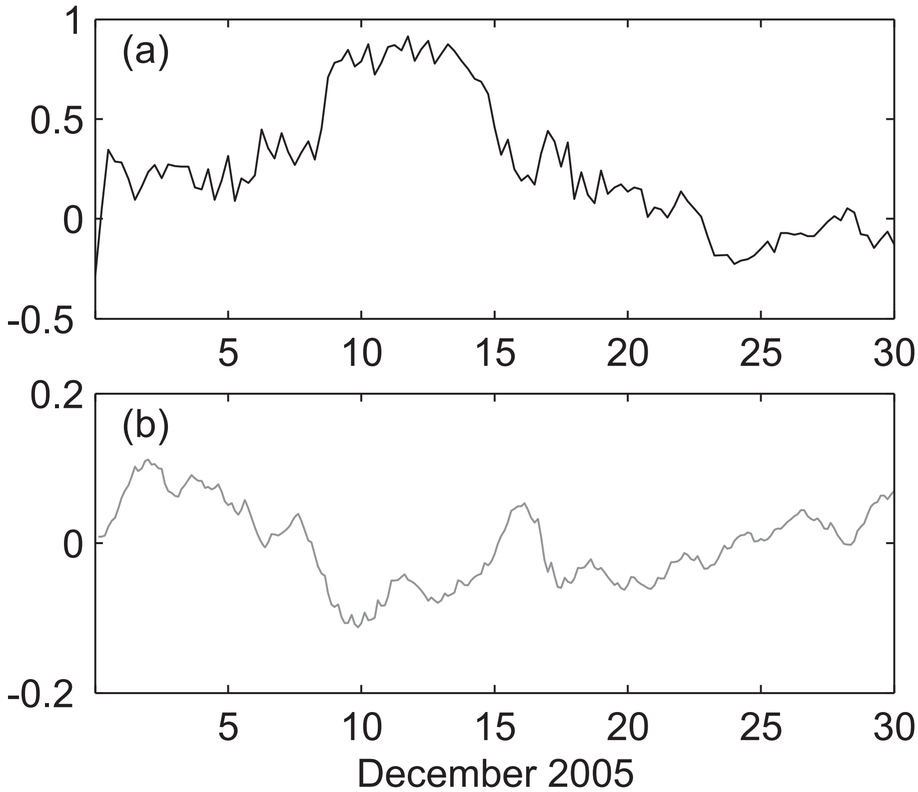

Fig. 10. (a) Total transport of volume (Sv) across the shelf break (200 m isobath) during December 2005. Positive values indicate transport from the shelf to open ocean. **(b)** Amplitude function of the most relevant EOF from the time variability of the u-component of wind forcing at 10 m.

OSD

3, 585–608, 2006

Operational analysis of NW Mediterranean shelf

A. Jordi et al.

EGU